

Extracting work from coherence in a two-mode Bose-Einstein condensate

L. A. Williamson,^{1,*} F. Cerisola,² J. Anders,^{2,3} and Matthew J. Davis^{1,†}

¹*ARC Centre of Excellence for Engineered Quantum Systems, School of Mathematics and Physics, University of Queensland, St Lucia, Queensland 4072, Australia*

²*Department of Physics and Astronomy, University of Exeter, Stocker Road, Exeter EX4 4QL, United Kingdom*

³*Institut für Physik und Astronomie, University of Potsdam, 14476 Potsdam, Germany*

(Dated: December 23, 2024)

We show how work can be extracted from number-state coherence in a two-mode Bose-Einstein condensate. With careful tuning of parameters, a sequence of thermodynamically reversible steps transforms a Glauber coherent state into a thermal state with the same energy probability distribution. The work extracted during this process arises entirely from the removal of quantum coherence. More generally, we characterise quantum (from coherence) and classical (remaining) contributions to work output, and find that in this system the quantum contribution can be dominant over a broad range of parameters. The proportion of quantum work output can be further enhanced by squeezing the initial state. Due to the many-body nature of the system, the work from coherence can equivalently be understood as work from entanglement.

I. INTRODUCTION

Converting disordered energy (heat) into ordered energy (work) is one of the most fundamental processes in thermodynamics. In a classical system, disorder arises from practical limitations on what can be known about a large system. Observables in a quantum system may exhibit not only classical uncertainty, but also quantum uncertainty arising from coherence [1, 2]. Quantum coherence is defined with respect to a particular basis, and occurs when a system exists in superpositions of eigenstates of that basis. Of particular relevance to thermodynamics is the quantum uncertainty in a system's energy, arising from coherence in the energy eigenbasis [3–5].

It is now well established that coherence in the energy eigenbasis can enhance work extraction if appropriately utilised. For a sufficiently rapid engine cycle, coherence can enhance power output beyond that of any classical engine operating with the same resources [6–8]. In single-shot realisations, coherence may diminish the maximum available work [9], however, a carefully chosen sequence of thermodynamic processes circumvents this degradation [10–13]. Despite the benefits of coherence in work extraction, protocols to realise these benefits in experimentally tractable systems are lacking. Such expositions are timely, considering the relevance to quantum information [14–16] and the growing field of quantum thermal machines [17, 18].

Bose-Einstein condensates (BECs) offer a pristine system in which to explore many-body quantum physics, due to a high degree of tuneability and isolation from the environment [19, 20]. In the field of quantum thermal machines, bosonic particle statistics can improve engine performance [21–24] and act as a fuel in an engine-like

cycle [25]. Interactions in a BEC can enhance engine performance [26, 27] or allow access to energetic degrees of freedom not available classically [28, 29]. However, the role of coherence in work extraction from a BEC has not been explored. Notably, two-mode BECs can exhibit long-lived coherence in the number state basis [30]. Incorporating squeezing [31–33], two-mode BECs can exhibit metrologically useful entanglement, allowing for quantum-enhanced measurement sensitivity [34–36].

In this manuscript we show how number-state coherence in a two-mode BEC can empower work extraction. To obtain work that is predominantly quantum in origin the initial state must be close to thermal when projected onto the energy eigenbasis. This is challenging in a quantum many-body system due to the exponentially large number of populations and coherences. We show that this challenge can be overcome by using a Glauber coherent state with mean boson number less than a critical value that depends on temperature. We introduce a formalism to quantify the work directly available from coherence and the work that would be available classically, and show that squeezing the initial state can substantially increase the proportion of quantum work extracted. The number-state coherence in our protocol arises from entangling correlations between the two modes of the BEC. Therefore the work extracted from coherence can equivalently be interpreted as work from entanglement, thus demonstrating the many-body nature of the protocol. To our knowledge, our work presents the first proposal showing how work can be extracted from coherence in a two-mode BEC, paving the way for experimental demonstration and highlighting the utility of two-mode BECs in thermodynamic applications.

* Corresponding author: lewis.williamson@uq.edu.au

† mdavis@uq.edu.au

II. BACKGROUND

A. Extracting work from coherence

To see how work can be extracted from quantum coherence generally, consider a Hamiltonian \hat{H} with thermal state $\rho_{\text{therm}} = e^{-\beta\hat{H}} / \text{Tr} e^{-\beta\hat{H}}$ at inverse temperature β . Now consider a second quantum state ρ that satisfies

$$\langle E_n | \rho | E_n \rangle = \langle E_n | \rho_{\text{therm}} | E_n \rangle, \quad (1)$$

with $|E_n\rangle$ the energy eigenstates of \hat{H} . The information entropy associated with energy measurements of state ρ (termed ‘‘energy entropy’’ in [5]) is

$$S^E = - \sum_n \langle E_n | \rho | E_n \rangle \ln \langle E_n | \rho | E_n \rangle, \quad (2)$$

which for an isolated system is non-decreasing under time evolution [37, 38]. When Eq. (1) is satisfied, the energy entropy of state ρ is identical to that of ρ_{therm} . If ρ is diagonal in the energy eigenbasis then S^E is equal to the von Neumann entropy $S^V = -\text{Tr}[\rho \ln \rho]$ and ρ is equal to ρ_{therm} , which is a completely passive state [39]. If, however, ρ contains coherences (off-diagonal) terms in the energy eigenbasis, S^E will differ from S^V [37, 40, 41]. The difference between the two,

$$S^E - S^V = \sum_{m,n \neq m} \langle E_m | \rho | E_n \rangle \langle E_n | \ln \rho | E_m \rangle, \quad (3)$$

can be extracted in the form of non-classical work [11, 13, 42]

$$W_{\text{quant}} = \beta^{-1}(S^E - S^V) = \beta^{-1}D(\rho || \rho_{\text{ed}}). \quad (4)$$

Here $D(\rho || \sigma) = \text{tr}[\rho \ln \rho] - \text{tr}[\rho \ln \sigma] \geq 0$ is the quantum relative entropy, and $\rho_{\text{ed}} = \sum_n \langle E_n | \rho | E_n \rangle |E_n\rangle \langle E_n|$ is the *projection* of the density matrix ρ onto the energy eigenstates (the ‘‘energy diagonal’’ density matrix). The quantity $D(\rho || \rho_{\text{ed}})$ is a monotonic measure of the quantum coherence of state ρ [43] and hence the work output, Eq. (4), is quantum in origin.

A protocol to extract work from coherence was presented in [11]. The efficacy of this protocol depends on how closely the system’s mean energy and energy entropy match that of the thermal state ρ_{therm} . When these match, any work extracted during the protocol is entirely from coherence. A sufficient condition for this matching is that $\rho_{\text{ed}} = \rho_{\text{therm}}$, Eq. (1). This can always be satisfied in a two-level system by choosing the temperature of ρ_{therm} to satisfy [44]

$$k_B T = \frac{E_1 - E_0}{\ln \frac{\langle E_0 | \rho | E_0 \rangle}{\langle E_1 | \rho | E_1 \rangle}}. \quad (5)$$

Here E_0 and E_1 are the two energy levels with $E_1 > E_0$.

In many-body systems, it is usually much harder to engineer experimentally a non-thermal state ρ satisfying

$\rho_{\text{ed}} = \rho_{\text{therm}}$. Achieving this requires

$$r_n = \frac{E_n - E_{n-1}}{\ln \frac{\langle E_{n-1} | \rho | E_{n-1} \rangle}{\langle E_n | \rho | E_n \rangle}}, \quad (6)$$

to be insensitive to n , in which case $k_B T = r_n$ [44, 45]. Engineering this for non-thermal many-body states ρ is often very difficult, since control of individual energy levels is usually not possible. As a result, the work output from coherence from such systems will be small. As we will show below, the energy-level structure of an interacting two-mode BEC allows $\rho_{\text{ed}} \approx \rho_{\text{therm}}$ for particular experimentally realisable initial states, hence allowing for work output with a high contribution from coherence.

B. System setup

We consider a two-mode BEC with fixed total boson number N . The two modes could be hyperfine spin states or spatial modes [46]. Number states of the system are denoted by $|n, k\rangle$, with n and $k = N - n$ the number of bosons in the two modes respectively. We denote the annihilation operators for the two modes by \hat{a} and \hat{b} , with $\hat{a}|n, k\rangle = \sqrt{n}|n-1, k\rangle$ and $\hat{b}|n, k\rangle = \sqrt{k}|n, k-1\rangle$. The Hamiltonian for the system is ($\hbar \equiv 1$ here and throughout) [35]

$$\begin{aligned} \hat{H} &= \omega_1 \hat{a}^\dagger \hat{a} + \omega_2 \hat{b}^\dagger \hat{b} + \frac{g_{11}}{2} \hat{a}^\dagger \hat{a}^\dagger \hat{a} \hat{a} + \frac{g_{22}}{2} \hat{b}^\dagger \hat{b}^\dagger \hat{b} \hat{b} \\ &\quad + g_{12} \hat{a}^\dagger \hat{b}^\dagger \hat{a} \hat{b} + E_0 \\ &\equiv \Delta \hat{a}^\dagger \hat{a} + g \hat{a}^\dagger \hat{a}^\dagger \hat{a} \hat{a}. \end{aligned} \quad (7)$$

Here ω_i is the single-particle energy and g_{ii} the interaction strength for modes $i = 1, 2$. We have also allowed for interactions between the two modes of strength g_{12} , for example if the two modes are spin states. The vacuum energy is E_0 . The operator $\hat{N} = \hat{a}^\dagger \hat{a} + \hat{b}^\dagger \hat{b}$ commutes with \hat{H} and hence the total boson number is conserved. In the second line of Eq. (7) we replace $\hat{b}^\dagger \hat{b}$ by $\hat{N} - \hat{a}^\dagger \hat{a}$ and define

$$\Delta \equiv \omega_1 - \omega_2 - (N-1)(g_{22} - g_{12}) \quad (8)$$

and

$$g \equiv \frac{g_{11} + g_{22} - 2g_{12}}{2}. \quad (9)$$

We choose $E_0 = -N\omega_2 - N(N-1)g_{22}/2$ so that $\hat{H}|0, N\rangle = 0$ for convenience. The choice of E_0 will not affect the net output of any cyclic process, for example the performance of an engine cycle. The detuning Δ for two spatial modes can be controlled via tuning the trapping potential [47], and for two spin states via tuning of a Zeeman field [48, 49]. As will be discussed below, we require thermal states that have a Gaussian (or approximately Gaussian) distribution over states $|n, N-n\rangle$, which requires $g > 0$. Hence the interaction

strengths must satisfy $g_{11} + g_{22} > 2g_{12}$, i.e. the average intramode interaction strength $(g_{11} + g_{22})/2$ must exceed the intermode interaction strength g_{12} . For two spatially separated modes we have $g_{12} = 0$ and therefore $g > 0$ is ensured as long as the intramode interactions g_{ii} are positive, as realised for example in ^{87}Rb and ^{23}Na condensates [50, 51].

Particle conservation confines the system to the subset of states $|n, N - n\rangle$. Since number states are eigenstates of Eq. (7), the number-state coherence realisable in a two-mode BEC [30] is equivalent to the energy coherence enabling work extraction, Eq. (3). The thermal state of \hat{H} is,

$$\rho_{\text{therm}} = \frac{1}{Z} e^{-\beta \hat{H}} = \sum_{n=0}^N p_n^{\text{therm}} |n, N - n\rangle \langle n, N - n|, \quad (10)$$

with

$$p_n^{\text{therm}} = \frac{1}{Z} e^{-\beta(gn(n-1) + \Delta n)} \quad (11)$$

the thermal occupation of state $|n, N - n\rangle$ and

$$Z = \sum_{n=0}^N e^{-\beta(gn(n-1) + \Delta n)} \quad (12)$$

the partition function. Due to particle interactions, the boson number distribution of a thermal state is approximately Gaussian (when $\beta g > 0$ and $-\beta \Delta \gg \sqrt{\beta g}$), in contrast to the Planck distribution of non-interacting bosons. This feature will be essential for the efficacy of our protocol as it will enable close matching between the initial and thermal boson number distributions. We assume $\beta g \ll 1$; noting that $gN \sim \mu$, where μ is the BEC chemical potential, this is ensured when $\beta \mu / N \ll 1$, a condition satisfied in most realisations of dilute gaseous BECs [52, 53]. We can then approximate the sum in Eq. (12) by an integral. We also assume $N \gg 1$ and $\langle \hat{a}^\dagger \hat{a} \rangle \ll N$, i.e. most of the particles are in the \hat{b} mode throughout the protocol. We can then set $N \rightarrow \infty$ and approximate $|n, N - n\rangle$ by a harmonic oscillator number state, which simplifies our calculations [54, 55]. Evaluating Eq. (12) with these two approximations gives

$$Z \approx \sqrt{\frac{\pi}{\beta g}} e^{\beta(g-\Delta)^2/(4g)} \left(\frac{1 + \text{erf}\left(\frac{\beta(g-\Delta)}{2\sqrt{\beta g}}\right)}{2} \right). \quad (13)$$

We denote the $N \rightarrow \infty$ approximation of $|n, N - n\rangle$ by $|n\rangle$ below, however it should be kept in mind that this state is an implicitly two-mode state.

III. RESULTS

Our objective is to find an experimentally realisable density matrix containing coherence in the energy eigenbasis with the same (or almost the same) energy and

energy entropy as a thermal state Eq. (11). As we will now argue, a Glauber coherent state (GCS) satisfies these criteria. A GCS is,

$$|\alpha\rangle = \hat{D}(\alpha) |0\rangle = \sum_{n=0}^{\infty} c_n |n\rangle, \quad (14)$$

with $\hat{D}(\alpha) = e^{\alpha \hat{a}^\dagger - \alpha^* \hat{a}}$ the displacement operator and $c_n = e^{-|\alpha|^2/2} \frac{\alpha^n}{\sqrt{n!}}$ [56]. Such a state can be realised via coherent rotation of a pure state $|0, N\rangle$ or $|N, 0\rangle$ [47, 57–61] or via interference measurements [62–64] (see also [65]), and gives rise to phase coherence between the two modes of the BEC [47, 66–70]. Note the upper limit of the sum in Eq. (14) is set to ∞ by assuming $|\alpha|^2 \ll N$ and $N \gg 1$ (see the discussion above Eq. (13)). A GCS is a superposition of energy eigenstates of Eq. (7) and hence $|\alpha\rangle \langle \alpha|$ contains off-diagonal terms $c_m^* c_n |n\rangle \langle m|$ ($m \neq n$); hence a GCS exhibits coherence with respect to the energy eigenbasis. The GCS number-state distribution $p_n^G = |c_n|^2$ is Poissonian with mean and variance equal to $|\alpha|^2$. For large $|\alpha|^2$ we have,

$$p_n^G = \frac{|\alpha|^{2n} e^{-|\alpha|^2}}{n!} \approx \frac{1}{\sqrt{2\pi|\alpha|^2}} e^{-(n-|\alpha|^2)^2/(2|\alpha|^2)}. \quad (15)$$

Choosing

$$|\alpha|^2 = \frac{g - \Delta}{2g}, \quad \beta g = \frac{1}{2|\alpha|^2}, \quad (16)$$

we obtain $p_n^G \approx p_n^{\text{therm}}$, with p_n^{therm} given by Eq. (11). Equivalently, it is easy to show that Eq. (6) is independent of n when $|\alpha|^2$ is chosen as in Eq. (16). Hence with precise tuning of parameters, as given in Eq. (16), work can be extracted from coherence as discussed in Sec. II A.

For more general parameters, the work output will have both a contribution from coherence and a ‘‘classical’’ contribution. Below we present an explicit protocol to show how work can be extracted from the coherence of a GCS. We then show how the work output depends on particle number and temperature, identifying a regime where the work output is dominated by the contribution from coherence. Next we show how the work output can be improved by squeezing the initial state and finally we discuss the role of entanglement in the system.

A. Protocol to extract work from a GCS

We begin in a GCS, Eq. (14), with Hamiltonian Eq. (7) and $\Delta = \Delta_0$. The energy of the initial state is $U_i = \langle \alpha | \hat{H} | \alpha \rangle = \Delta_0 |\alpha|^2 + g |\alpha|^4$. To extract work from the GCS we consider the following thermodynamically reversible steps [11] (see Fig. 1):

1. Coherently couple the two modes of the BEC via the Hamiltonian $\kappa(\hat{b}^\dagger \hat{a} + \hat{a}^\dagger \hat{b})$, with $\kappa > 0$ the coupling rate. Evolve the system so that $|\alpha\rangle$ is displaced to $|0\rangle$ and all particles are in the \hat{b} mode.

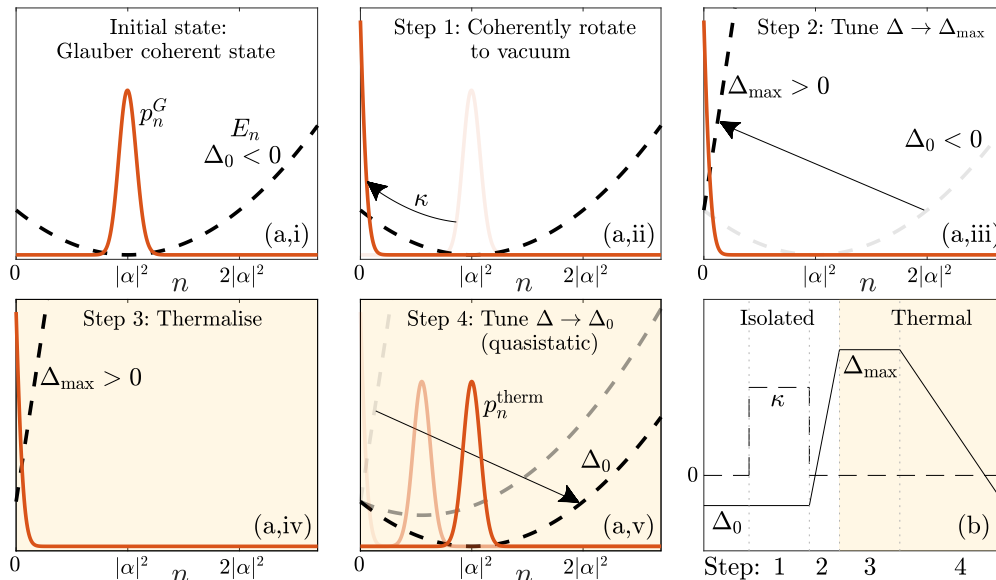


FIG. 1. (a) Protocol to extract work from coherence in a two-mode BEC. Red curves are number state distributions $\langle n|\rho|n\rangle$ and black dashed curves are the energy spectrum E_n , both smoothed over the discrete variable n . (a,i) The system is initialised in a Glauber coherent state (GCS) at detuning Δ_0 with mean boson number $|\alpha|^2 \gg 1$ and number distribution p_n^G , Eq. (15). The energy spectrum has a minimum at $n_{\min} = \max(0, (g - \Delta_0)/2)$; we choose $\Delta_0 < 0$ in the schematic above so that $n_{\min} > 0$. (a,ii) Step 1: Work is exchanged as the system is rotated to the vacuum state via a coherent coupling κ . (a,iii) Step 2: The detuning is changed to $\Delta_{\max} \gg \beta^{-1}$. The new energy spectrum has a minimum at $n = 0$ with an energy spacing much larger than β^{-1} . Hence the vacuum state is approximately thermal. (a,iv) Step 3: The system is coupled to a reservoir at inverse temperature β (indicated by background colouring). (a,v) Step 4: Work is extracted isothermally as the detuning is quasistatically adjusted to its initial value Δ_0 . The closeness of the final thermal distribution p_n^{therm} to the initial distribution p_n^G determines the quantum and classical contributions to the total work extracted in steps 1-4. The classical contribution can be suppressed with careful tuning of parameters, in which case the work extracted arises entirely from the initial energy coherence. (b) Detuning (solid line) and the coherent coupling (dashed line) between the two modes of the BEC during the steps in (a).

During this step, coherence is removed and work U_i is exchanged with the coupling field over a time scale κ^{-1} . Turn off the coupling κ so that the system energy is determined by Eq. (7).

2. Tune the detuning to $\Delta_{\max} > 0$. This does not change the system energy since the system is in state $|0\rangle$.
3. Couple the system to a reservoir at inverse temperature β and allow to thermalise. The detuning Δ_{\max} and β are chosen to satisfy $\beta\Delta_{\max} \gg 1$. Occupation of modes $|n\rangle$ with $n > 0$ are therefore thermally suppressed (see Eq. (12)) and hence $|0\rangle$ is approximately the thermal state. The energy increase during thermalisation is $\approx \Delta_{\max} e^{-\beta\Delta_{\max}}$ and is hence negligible for $\beta\Delta_{\max} \gg 1$.
4. Quasistatically change the detuning back to Δ_0 such that the system remains in thermal equilibrium with the reservoir throughout. Work is extracted and heat is absorbed in this step. The final state is thermal with energy $U_f = -\partial \ln Z / \partial \beta$ evaluated from Eq. (13) with $\Delta = \Delta_0$.

The coherent coupling in the first step could be achieved using Josephson oscillations for two spatial modes [47, 59] or via a Rabi pulse for two spin states [60, 61]. Complete conversion is possible when κ is much larger than the other energy scales in the problem, which ensures the dynamics is in the Josephson regime, rather than the self-trapping regime [46, 57, 58, 71]. Note the effect of changing Δ in steps 2-4 could also be achieved by manipulating g using a Feshbach resonance [72–74] with Δ fixed: g would be increased to a value $\beta g_{\max} \gg 1$ in steps 2 and 3 and then quasistatically reduced back to its initial value in step 4. This alternative protocol would not change the results below.

The total mean work output from the protocol in Fig. 1 is [11]

$$W = U_i - U_f - \beta^{-1}(S_i^V - S_f^V), \quad (17)$$

where $S_i^V(S_f^V)$ are the initial (final) von Neumann entropies of the system.

For the protocol in Fig. 1 we have $S_i^V = 0$ since the initial state is pure and $S_f^V = S_f^E$ since the final state is thermal. Here $S_i^E(S_f^E)$ are the energy entropies for the initial (final) state. The total entropic change $S_f^V - S_i^V$

can now be decomposed into a classical contribution $S_f^E - S_i^E$ and a quantum contribution $S_i^E - S_i^V = D(\rho||\rho_{\text{ed}})$ arising from coherence, Eq. (3). The work then consists of two parts [11, 13, 75], a quantum part as defined in Eq. (4), as well as a classical part:

$$\begin{aligned} W_{\text{quant}} &= \beta^{-1}(S_i^E - S_i^V) \\ W_{\text{class}} &= U_i - U_f - \beta^{-1}(S_i^E - S_f^E). \end{aligned} \quad (18)$$

Note that a projection of the initial state Eq. (14) onto the energy eigenbasis prior to work extraction, i.e. $\rho \rightarrow \rho_{\text{ed}}$, would result in $W_{\text{quant}} = 0$, but would not change W_{class} . The protocol in Fig. 1 avoids such projection, allowing W_{quant} to be extracted.

B. Classical and quantum contributions to the work extracted from a GCS

With an initial state (14), the outputs W_{quant} and W_{class} in Eq. (18) can be calculated analytically. We choose $|\alpha\rangle$ so that the GCS has mean boson number equal to the thermal state,

$$|\alpha|^2 = \langle \hat{n} \rangle_{\text{therm}} \equiv \langle \hat{n} \rangle. \quad (19)$$

Here $\hat{n} = \hat{a}^\dagger \hat{a}$ and a ‘‘therm’’ subscript denotes expectation values for state ρ_{therm} , Eq. (10). We have checked that this choice of $|\alpha\rangle$ minimises W_{class} to a very good approximation over the parameters explored. The energetic and entropic terms in Eq. (18) are

$$\begin{aligned} U_i - U_f &= g(\langle \hat{n} \rangle - \langle \delta \hat{n}^2 \rangle_{\text{therm}}), \\ S_i^E &= \frac{1}{2} + \frac{1}{2} \ln(2\pi \langle \hat{n} \rangle) + O\left(\frac{1}{\langle \hat{n} \rangle}\right), \\ S_f^E &= \frac{1}{2} + \frac{1}{2} \ln(2\pi \langle \delta \hat{n}^2 \rangle_{\text{therm}}) + S_{\text{NG}}, \end{aligned} \quad (20)$$

where $\langle \delta \hat{n}^2 \rangle = \langle \hat{n}^2 \rangle - \langle \hat{n} \rangle^2$. We have also introduced

$$S_{\text{NG}} = \ln \frac{1 + \text{erf } u}{2} - uG(u) - \ln[1 - 2uG(u) - 2G(u)^2], \quad (21)$$

with $u = \frac{\beta(g - \Delta_0)}{2\sqrt{\beta g}}$ and $G(u) = \frac{e^{-u^2}}{\sqrt{\pi}(1 + \text{erf } u)} = O(e^{-\beta \Delta_0^2 / (4g)})$. The entropic correction S_{NG} arises since the thermal distribution is not a perfect Gaussian, and is only important for $u \lesssim 1$.

The thermal mean and variance are

$$\langle \hat{n} \rangle_{\text{therm}} = \frac{1}{\sqrt{\beta g}} (u + G(u)), \quad (22)$$

$$\langle \delta \hat{n}^2 \rangle_{\text{therm}} = \frac{1}{2\beta g} (1 - 2uG(u) - 2G(u)^2). \quad (23)$$

Again, the $G(u)$ terms are non-Gaussian corrections, which are only important for $u \lesssim 1$. Note for $u \gg 1$

we have $u^2 \approx \langle \hat{n} \rangle_{\text{therm}}^2 / (2\langle \delta \hat{n}^2 \rangle_{\text{therm}})$ and hence u^{-1} is essentially the normalized second-order correlation function of the thermal bosonic field [76]. The thermal mean, variance and third central moment $\langle \delta \hat{n}^3 \rangle = \langle (\hat{n} - \langle \hat{n} \rangle)^3 \rangle$ are shown in the inset to Fig. 2(a). We focus on cases $\langle \hat{n} \rangle_{\text{therm}} \gtrsim 1$, which is ensured when the initial detuning is less than the reservoir temperature,

$$-\infty < \beta \Delta_0 \lesssim 1. \quad (24)$$

We hence allow $\beta \Delta_0$ to be negative. This is easy to engineer in a two-mode BEC but difficult to engineer in other bosonic systems that do not have a constrained particle number, e.g. photons.

Analytic expressions for W_{class} and W_{quant} follow from Eq. (18)–(23) and are plotted in Fig. 2(a) as a function of $\langle \hat{n} \rangle$. Note $\langle \hat{n} \rangle$ is itself a function of Δ_0 , according to Eq. (22), and hence varying $\langle \hat{n} \rangle$ corresponds to an implicit variation of Δ_0 . The minimum of the classical work occurs when p_n^G and p_n^{therm} are as close as possible, see Fig. 2(b). For large $\langle \hat{n} \rangle$ both distributions are approximately Gaussian and hence will be equal when their respective means and variances are equal. Since p_n^G has equal mean and variance, this requires

$$|\alpha|^2 = \langle \hat{n} \rangle_{\text{therm}} = \langle \delta \hat{n}^2 \rangle_{\text{therm}}. \quad (25)$$

This occurs when $\beta \Delta_0 \approx -1$, at which point $\langle \hat{n} \rangle_{\text{therm}} = \langle \delta \hat{n}^2 \rangle_{\text{therm}} \approx 1/(2\beta g)$. At this optimal point, $W_{\text{class}} = O(\langle \hat{n} \rangle^{-1})$ and the work output almost exclusively consists of W_{quant} . (Note our choice of units: plotting work in units of β^{-1} is equivalent to plotting the information lost if the work was dissipated as heat, according to Landauer’s principle [77].)

For $\langle \hat{n} \rangle \neq \langle \delta \hat{n}^2 \rangle_{\text{therm}}$, the protocol is suboptimal in the sense that W_{class} is no longer approximately zero. Here the thermal bosons are either bunched or anti-bunched, caused by the boson interactions [78]. For $\langle \hat{n} \rangle > \langle \delta \hat{n}^2 \rangle_{\text{therm}}$ (thermal anti-bunching), large number fluctuations in the initial state result in a large $U_i - U_f$, see Fig. 2(b). In this regime, $u \gg 1$ and Eq. (20)–(23) simplify to give

$$\begin{aligned} W_{\text{class}} &\approx g \langle \hat{n} \rangle - \frac{1}{2\beta} - \frac{1}{2\beta} \ln(2\beta g \langle \hat{n} \rangle), \\ W_{\text{quant}} &\approx \frac{1}{2\beta} + \frac{1}{2\beta} \ln(2\pi \langle \hat{n} \rangle). \end{aligned} \quad (u \gg 1) \quad (26)$$

Using Eq. (26), we find that $W_{\text{quant}} > W_{\text{class}}$ for

$$\langle \hat{n} \rangle \lesssim \frac{1}{\beta g} \left[-\Omega_{-1} \left(-\sqrt{\frac{\beta g}{4\pi \exp(2)}} \right) \right] \equiv n_G, \quad (27)$$

see Fig. 2(a). Here Ω_k is the k th branch of the omega function [79]. The function $-\Omega_{-1}(-x)$ satisfies $1 \leq -\Omega_{-1}(-x) < \infty$ for $x \in (0, \exp(-1)]$ and monotonically decreases with increasing x , with $-\Omega_{-1}(-x) \sim \ln(\frac{1}{x} \ln \frac{1}{x})$ for small x [80]. Hence, ignoring logarithmic

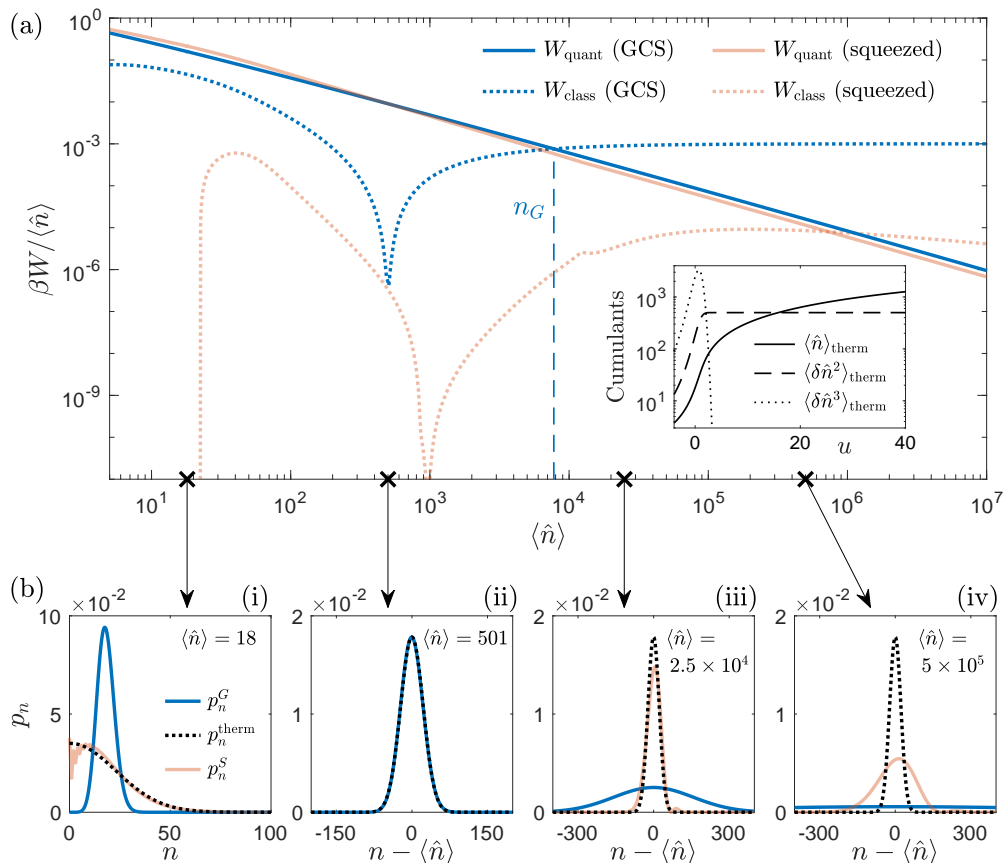


FIG. 2. (a) Work extracted from a two-mode BEC undergoing the protocol in Fig. 1 for different mean bosonic numbers $\langle \hat{n} \rangle$. Work extracted from an initial GCS (blue curves) divided into quantum βW_{quant} (blue solid curve) and classical βW_{class} (blue dotted curve) contributions, see Eq. (18). The work output is dominated by W_{quant} for $\langle \hat{n} \rangle \lesssim n_G$, with n_G given by Eq. (27) and marked by a vertical dashed line. The number state distributions for the GCS and thermal states coincide almost perfectly when $\langle \hat{n} \rangle = 1/(2\beta g)$, at which point $W_{\text{class}} \approx 0$ is minimised (dip in blue dotted curve). Inset: First three cumulants of the thermal boson number distribution, with $\langle \delta \hat{n}^k \rangle = \langle (\hat{n} - \langle \hat{n} \rangle)^k \rangle$ for $k = 2, 3$. The distribution is Gaussian for $u \gg 1$, in which case $\langle \hat{n} \rangle_{\text{therm}} \approx u/\sqrt{\beta g}$, $\langle \delta \hat{n}^2 \rangle_{\text{therm}} \approx 1/(2\beta g)$ and higher order cumulants are zero. (b) (i)-(iv) Number state distributions for different mean bosonic numbers (four panel values are marked by crosses in (a)) for a GCS (blue curve) and a thermal state (black dashed curve). The GCS distribution is narrower (wider) than the thermal distribution for $\langle \hat{n} \rangle$ smaller (larger) than $\langle \delta \hat{n}^2 \rangle_{\text{therm}} \approx 1/(2\beta g) \approx 501$, which results in non-zero W_{class} . Pale red curves in (a) and (b): as for the GCS but for a squeezed state. These are included here for comparison and will be discussed in Sec. III C. The GCS and squeezed distributions coincide in (ii). All results are for $\beta g = 10^{-3}$. Different $\langle \hat{n} \rangle$ correspond to different $\beta \Delta_0$, which in (b) are: (i) $-\beta \Delta_0 = 0$, (ii) $-\beta \Delta_0 = 1$, (iii) $-\beta \Delta_0 = 50$, (iv) $-\beta \Delta_0 = 10^3$.

corrections, n_G decreases with increasing βg as $n_G \sim 1/(\beta g)$. For $\langle \hat{n} \rangle > n_G$, the classical work output grows extensively due to the extensive growth of $U_i - U_f$, see Eq. (26). The quantum work also increases with $\langle \hat{n} \rangle$ due to increased coherence in the initial state. The increase, however, is subextensive, with $W_{\text{quant}} \sim \frac{1}{2\beta} \ln \langle \hat{n} \rangle$. For $\langle \hat{n} \rangle < \langle \delta \hat{n}^2 \rangle_{\text{therm}}$ (thermal bunching), the number fluctuations of the initial state are less than the final state, see Fig. 2(b). Although this increases W_{class} , we still have $W_{\text{quant}} > W_{\text{class}}$ as long as $\langle \hat{n} \rangle \gg 1$, see Fig. 2(a).

C. Improved protocol using squeezing

The boson number distribution of a GCS is Poissonian, and hence the mean and variance are always equal. For sufficiently large mean boson number, Eq. (27), the work output becomes dominated by W_{class} . The classical work output can be suppressed much more effectively by using a squeezed initial state. Squeezing of a two-mode BEC is possible using multiple techniques [35, 81], including time evolution with a one-axis twisting Hamiltonian [33, 82, 83] and parametric downconversion via spin-changing collisions [84–86]. A displaced squeezed state is [87–89],

$$|\alpha, \zeta\rangle = \hat{D}(\alpha) \hat{S}(\zeta) |0\rangle, \quad (28)$$

where $\hat{S}(\zeta) = e^{(\zeta^* \hat{a} \hat{a} - \zeta \hat{a}^\dagger \hat{a}^\dagger)/2}$ is the squeezing operator and $\zeta = |\zeta| e^{i\theta}$ parameterises the squeezing. The distribution $p_n^S = |\langle n|\alpha, \zeta\rangle|^2$ is [90, 91]

$$p_n^S = \frac{\left(\frac{1}{2} \tanh |\zeta|\right)^n}{n! \cosh |\zeta|} |H_n(\lambda\alpha)|^2 e^{-\alpha^2(1+\cos\theta \tanh |\zeta|)}, \quad (29)$$

with H_n the Hermite polynomials ($H_0(x) = 1$, $H_1(x) = 2x$, etc.) and

$$\lambda = \frac{e^{-i\theta/2} \cosh |\zeta| + e^{i\theta/2} \sinh |\zeta|}{\sqrt{\sinh 2|\zeta|}}. \quad (30)$$

The boson number distribution for a squeezed state can have a variance smaller or larger than its mean, controllable via the squeezing parameter ζ . This additional control allows the initial number distribution to be matched more closely to p_n^{therm} , see Fig. 2(b). The work output from an initial squeezed state is compared with that of a GCS in Fig. 2(a). Squeezing suppresses W_{class} over a much larger range of $\langle \hat{n} \rangle$ compared to the GCS. Note the small but finite minimum of $W_{\text{class}}/\langle \hat{n} \rangle$ for a GCS, which arises due to the approximation in Eq. (15), is reduced even further by squeezing, see Fig. 2(a). Further squeezed results are shown in Fig. 3(a) for different values of βg . For the squeezed state, we choose $|\alpha|^2$ so that the mean boson number is equal to that of the thermal state and choose ζ to minimise differences in higher order moments. Details are discussed in Appendix A and the values of $|\zeta|$ and $\cos\theta$ obtained are plotted in Fig. 3(b). Numerical details to obtain p_n^S are described in Appendix B.

Although squeezing gives much greater control over the initial boson number distribution, its variance is still constrained by $\langle \hat{n} \rangle$ [92]. For large $\langle \hat{n} \rangle$ the minimum variance possible for a squeezed state is (see Appendix C)

$$\min \langle \delta \hat{n}^2 \rangle \approx \left(\frac{27}{32}\right)^{1/3} \langle \hat{n} \rangle^{2/3} \quad (31)$$

Achieving $\langle \delta \hat{n}^2 \rangle = \langle \delta \hat{n}^2 \rangle_{\text{therm}}$ is hence only possible when the mean boson number is not too large,

$$\langle \hat{n} \rangle \leq \sqrt{\frac{32 \langle \delta \hat{n}^2 \rangle_{\text{therm}}^3}{27}} \approx \sqrt{\frac{4}{27(\beta g)^3}}. \quad (32)$$

The constraint (32) should be contrasted with the strict constraint for a GCS, Eq. (25). Matching the mean and variances of p_n^S and p_n^{therm} gives $U_i = U_f$ and hence $W_{\text{class}} = \beta^{-1}(S_f^E - S_i^E)$, see Eq. (18).

If the mean boson number is too large such that Eq. (32) is not satisfied, the variance of the squeezed distribution cannot be made small enough to match $\langle \delta \hat{n}^2 \rangle_{\text{therm}}$. We then choose $\langle \delta \hat{n}^2 \rangle$ to take on its minimum value Eq. (31) by choosing $e^{-2|\zeta|} = (4\langle \hat{n} \rangle)^{-1/3}$ (see Appendix C). This results in subextensive scaling of W_{class} for large $\langle \hat{n} \rangle$,

$$W_{\text{class}} \sim g \left(\frac{27}{32}\right)^{1/3} \langle \hat{n} \rangle^{2/3}, \quad (33)$$

see Fig. 3(a). Notably, this contrasts the extensive scaling of W_{class} for a GCS, which arises from the strict constraint $\langle \hat{n} \rangle = \langle \delta \hat{n}^2 \rangle$, see Fig. 2(a) and Eq. (26). For large $\langle \hat{n} \rangle$, we find W_{quant} is well approximated by

$$W_{\text{quant}} \approx \frac{1}{2\beta} + \frac{1}{2\beta} \ln \left[2\pi \left(\frac{27}{32}\right)^{1/3} \langle \hat{n} \rangle^{2/3} \right], \quad (34)$$

see Fig. 3(a). This follows from approximating p_n^S by a Gaussian distribution and using Eq. (31). Equations (33) and (34) give the following criteria for $W_{\text{quant}} > W_{\text{class}}$,

$$\langle \hat{n} \rangle \lesssim \sqrt{\frac{32}{27} n_G^3} \equiv n_S, \quad (35)$$

with n_G the equivalent bound for a GCS given by Eq. (27). The estimate Eq. (35) agrees well with our numerics, see Fig. 3(a). Notably, $n_S \gg n_G$ for large n_G .

For small $\langle \hat{n} \rangle$, we observe an abrupt drop in W_{class} , see Fig. 3(a). At this point, S_i^E increases above S_f^E and hence W_{class} becomes negative ($W_{\text{class}} = S_f^E - S_i^E$ for small $\langle \hat{n} \rangle$, see Eq. (32)). We expect that the increase in S_i^E above S_f^E is due to oscillations that arise in the squeezed distribution for small $\langle \hat{n} \rangle$ [93, 94], see Fig. 2(b) [95].

D. Relation with entanglement

Finally, we show how the work from coherence in this system can equivalently be interpreted as work from entanglement [96–99]. To see this, we evaluate the entanglement entropy \mathcal{S} between the two modes of the BEC. A sufficient condition for entanglement is then $\mathcal{S} > 0$ [100]. The entanglement entropy of a pure state ρ is

$$\mathcal{S} = -\text{Tr}_1 \rho_1 \log \rho_1, \quad (36)$$

where $\rho_1 = \text{Tr}_2 \rho$ and Tr_i is a partial trace over boson states of modes $i = 1, 2$. The trace Tr_2 can be evaluated in the number state basis for both modes. Due to conservation of total particle number, this projects ρ onto the number state basis for the first mode,

$$\rho_1 = \sum_{n=0}^N \langle n, N-n | \rho | n, N-n \rangle |n\rangle_1 \langle n| \quad (37)$$

with $|n\rangle_1 \langle n| = \text{Tr}_2 |n, N-n\rangle \langle n, N-n|$. The “1” subscript distinguishes $|n\rangle_1$ from the implicitly two-mode state $|n\rangle$. Equations (36) and (37) give

$$\mathcal{S} = S_i^E = \beta W_{\text{quant}}. \quad (38)$$

Hence the coherence in this system arises due to entangling correlations between the two modes, which is subsequently extracted as W_{quant} . The final thermal state is a classical mixture of product states, and hence does not possess any entanglement. The quantum work output from coherence can therefore equivalently be interpreted as work from entanglement. Squeezing results in additional entanglement according to the criteria in [32, 101].

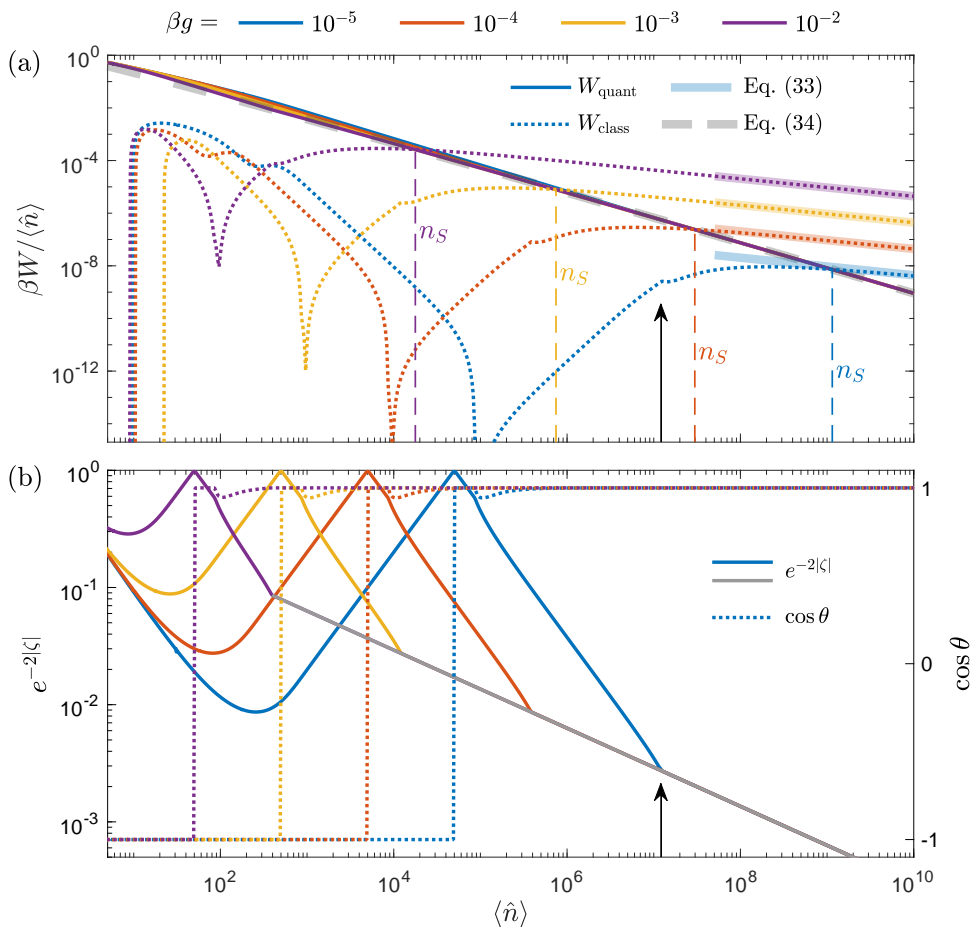


FIG. 3. (a) Work extracted from an initial squeezed state, divided into quantum βW_{quant} (solid curves) and classical βW_{class} (dotted curves) contributions. Colours indicate different values of βg . The work output is dominated by W_{quant} for $\langle \hat{n} \rangle \lesssim n_S$, with n_S given by Eq. (35) and marked by vertical dashed lines. Lighter-coloured thicker lines give the large $\langle \hat{n} \rangle$ result for W_{class} , Eq. (33), demonstrating subextensive scaling of W_{class} . Grey dashed line gives the large $\langle \hat{n} \rangle$ result for W_{quant} , Eq. (34). (b) Optimised squeezing parameters $e^{-2|\zeta|}$ (solid curves, left axis) and $\cos \theta$ (dotted curves, right axis) for the squeezed state (see text for details). For $\langle \hat{n} \rangle \leq 2(3\beta g)^{-3/2}$ the squeezed variance can be matched to the thermal variance with appropriate choice of $e^{-2|\zeta|}$. For larger $\langle \hat{n} \rangle$ matching is no longer possible, see Eq. (32); minimising the squeezed variance then gives $e^{-2|\zeta|} = (4\langle \hat{n} \rangle)^{-1/3}$ (gray line), independent of βg . This results in a discontinuity in the slope of $e^{-2|\zeta|}$ and W_{class} at $\langle \hat{n} \rangle = 2(3\beta g)^{-3/2}$ (marked by vertical arrows for $\beta g = 10^{-5}$).

IV. DISCUSSION AND CONCLUSION

We have shown how work can be extracted from coherence in a two-mode BEC. Work almost entirely from coherence can be extracted from a GCS with precisely tuned mean boson number. The protocol can be substantially improved using squeezing, enabling work extraction predominantly from coherence over a much broader range of parameters. Due to the many-body nature of the system, the work from coherence can equivalently be interpreted as work from entanglement.

The coherent steps in our protocol can be realised in current experiments with two-mode BECs, which could be spatial or spin modes [46]. For two spatial modes the detuning can be controlled by varying trap depth [47] and

populations can be coherently controlled using Josephson oscillations [47, 59]. For two spin states the detuning can be controlled using Zeeman fields [48, 49] and populations can be controlled using a Rabi pulse [60, 61]. The effect of changing Δ in the protocol could also be achieved by manipulating g using a Feshbach resonance [72–74]. Squeezing of a two-mode BEC can be realised using a variety of techniques [33, 35, 81–86]. Our protocol requires $\beta g \ll 1$, which is satisfied in most realisations of dilute gaseous BECs [52, 53].

The experimentally challenging part of the protocol is the thermalisation of the system with a reservoir (step 3 in Fig. 1). This could potentially be achieved by immersing the system in a thermal quantum gas of another species, in analogy with sympathetic cooling [102]. An

optical tweezer trap would allow the system to be moved in and out of the reservoir as needed. Particle exchange between the two modes during thermalization could occur via tunnelling for two spatial modes [103, 104] or via spin-changing collisions with the reservoir for two spin states [105–108]. We have assumed decoherence only occurs during the thermalising step of our protocol. Additional decoherence will likely reduce the work output by a term that scales linearly with the irreversible entropy production [75].

The Hamiltonian Eq. (7) also describes a large, fully-connected spin chain [109] and hence could be realised in other atomic systems [35], including atomic ensembles coupled to light [110, 111], Rydberg arrays [112, 113] and trapped ions [114, 115]. The Hamiltonian also resembles that of photons in a non-linear medium [90], with the important difference that we allow the free-photon spectrum to be negative, $\Delta < 0$. To realise this, photon number would need to be conserved [116, 117].

We have limited our analysis to Glauber coherent and squeezed states. Improved operation may be possible using self-phase modulation of the squeezed state [118] or by using non-Gaussian states [119] at the expense of more involved state generation. We have also limited our analysis to initial states with zero von Neumann entropy; relaxing this provides an interesting area for future investigation. Extracting work from coherence can enhance power output compared to classical systems [6]. Our results provide a starting point to explore this in a two-mode BEC, and may result in a many-body quantum advantage when incorporated into an engine cycle.

DATA AVAILABILITY

The code used to produce the data shown in Figs. 2 and 3 is available upon reasonable request to LW, lewis.williamson@uq.edu.au.

ACKNOWLEDGEMENTS

This research was supported by the Australian Research Council Centre of Excellence for Engineered Quantum Systems (EQUS, CE170100009) and the Australian government Department of Industry, Science, and Resources via the Australia-India Strategic Research Fund (AIRXIV000025). FC and JA gratefully acknowledge funding from the Foundational Questions Institute Fund (FQXi-IAF19-01) and EPSRC (EP/R045577/1). JA thanks the Royal Society for support.

Appendix A: Choosing squeezing parameters

We choose α and ζ for the initial squeezed state as follows. The first three cumulants of p_n^S are evaluated

from the generating function $K(s) = \ln \sum_n p_n^S e^{sn}$, which can be written in closed form using Mehler's formula [120]

$$\sum_{n=0}^{\infty} \frac{H_n(x)H_n(y)}{n!} \left(\frac{u}{2}\right)^n = \frac{1}{\sqrt{1-u^2}} e^{\frac{2xyu - (x^2+y^2)u^2}{1-u^2}}. \quad (\text{A1})$$

This gives

$$\begin{aligned} \langle \hat{n} \rangle &= \sinh^2 |\zeta| + |\alpha|^2, \\ \langle \delta \hat{n}^2 \rangle &= 2 \cosh^2 |\zeta| \sinh^2 |\zeta| + |\alpha|^2 (\cosh(2|\zeta|) - \sinh(2|\zeta| \cos \theta)), \\ \langle \delta n^3 \rangle &= \cosh(2|\zeta|) \sinh^2(2|\zeta|) \\ &\quad + \frac{3|\alpha|^2}{2} \left(\cosh(4|\zeta|) - \frac{1}{3} - \sinh(4|\zeta| \cos \theta) \right), \end{aligned} \quad (\text{A2})$$

with $\langle \delta n^k \rangle = \langle (n - \langle \hat{n} \rangle)^k \rangle$ for $k = 2, 3$. We set $\langle \hat{n} \rangle = \langle \hat{n} \rangle_{\text{therm}}$ by choosing $|\alpha|^2 = \langle \hat{n} \rangle_{\text{therm}} - \sinh^2 |\zeta|$. We solve for $|\zeta|$ by minimising $|\langle \delta n^2 \rangle - \langle \delta \hat{n}^2 \rangle_{\text{therm}}|$. Since the Hamiltonian (7) depends only on $\langle \hat{n} \rangle$ and $\langle \delta \hat{n}^2 \rangle$, this choice minimises $|U_f - U_i|$. Additionally, for not-too-large squeezing this minimises $|S_f^E - S_i^E|$. We then choose $\cos \theta$ to minimise $|\langle \delta n^3 \rangle|$.

Appendix B: Numerical details for extracting squeezed state statistics

Numerical computation of p_n^S requires care for large n due to numerical overflow and underflow [121]. We evaluate p_n^S using the underlying recursion relation [90, 91] $c_n = \langle n | \alpha, \zeta \rangle = \frac{\alpha(1+e^{i\theta} \tanh |\zeta|)}{\sqrt{n}} c_{n-1} - e^{i\theta} \tanh |\zeta| \sqrt{\frac{n-1}{n}} c_{n-2}$. After each iteration we normalise the distribution. Defining $\Delta n = \text{ceil}(50\sqrt{\langle \delta \hat{n}^2 \rangle})$, we begin the recursion at $n^* = \max(0, \text{round}(\langle \hat{n} \rangle - \Delta n/2))$ with $c_{n^*} = 1$ and $c_{n < n^*} = 0$, and evaluate terms up to $n^* + \Delta n$. In cases where $n^* > 0$, we find $|\alpha| \gg 1$ and hence $c_{n^*+1} \approx \frac{\alpha(1+e^{i\theta} \tanh |\zeta|)}{\sqrt{n^*}} c_{n^*}$ (this is exact for $n^* = 0$). Hence why the values of $c_{n < n^*}$ are not needed.

Appendix C: Minimum variance of a squeezed state

To a very good approximation $\cos \theta = \pm 1$, see Fig. 3(b). Defining $x = e^{2|\zeta| \cos \theta} (= e^{\pm 2|\zeta|})$, the equation for $\langle \delta \hat{n}^2 \rangle$ is (see Eq. (A2)),

$$\langle \delta \hat{n}^2 \rangle = \frac{1}{8x^2} \left(x^4 - 4x^2 + 8 \left(\langle \hat{n} \rangle + \frac{1}{2} \right) x - 1 \right). \quad (\text{C1})$$

Stationary points of $d\langle \delta \hat{n}^2 \rangle / dx$ satisfy the polynomial

$$x^4 - 4 \left(\langle \hat{n} \rangle + \frac{1}{2} \right) x + 1 = 0. \quad (\text{C2})$$

Equation (C2) can be solved for x using standard methods. For large $\langle \hat{n} \rangle$ this gives two real roots and two complex roots. The two real roots are

$$\begin{aligned} x_1 &\approx \frac{1}{4\langle \hat{n} \rangle + 2}, \\ x_2 &\approx (4\langle \hat{n} \rangle)^{1/3}, \end{aligned} \quad (\text{C3})$$

with x_1 corresponding to a local maximum of Eq. (C1) and $x_2 > x_1$ a local minimum. Substituting $x \leq x_1$ into the expression for $\langle \hat{n} \rangle$ (Eq. (A2)) would give a negative value for $|\alpha|^2$, hence $x > x_1$. Therefore x_2 gives the global minimum of $\langle \delta \hat{n}^2 \rangle$ for valid values of x . Substituting x_2 into Eq. (C1) gives Eq. (31) for large $\langle \hat{n} \rangle$.

For the purpose of open access, the authors have applied a ‘Creative Commons Attribution’ (CC BY) licence to any Author Accepted Manuscript version arising from this submission.

-
- [1] J. Åberg, Quantifying superposition, arXiv:quant-ph/0612146 (2006).
- [2] A. Streltsov, G. Adesso, and M. B. Plenio, Colloquium: Quantum coherence as a resource, *Rev. Mod. Phys.* **89**, 041003 (2017).
- [3] S. Vinjanampathy and J. Anders, Quantum thermodynamics, *Contemp. Phys.* **57**, 545 (2016).
- [4] J. Goold, M. Huber, A. Riera, L. Del Rio, and P. Skrzypczyk, The role of quantum information in thermodynamics—a topical review, *J. Phys. A: Math. Theor.* **49**, 143001 (2016).
- [5] F. Binder, L. A. Correa, C. Gogolin, J. Anders, and G. Adesso, eds., *Thermodynamics in the Quantum Regime — Fundamental Aspects and New Directions* (Springer Nature Switzerland, Cham, 2018).
- [6] R. Uzdin, A. Levy, and R. Kosloff, Equivalence of quantum heat machines, and quantum-thermodynamic signatures, *Phys. Rev. X* **5**, 031044 (2015).
- [7] R. Uzdin, Coherence-induced reversibility and collective operation of quantum heat machines via coherence recycling, *Phys. Rev. Appl.* **6**, 024004 (2016).
- [8] J. Klatzow, J. N. Becker, P. M. Ledingham, C. Weinzetl, K. T. Kaczmarek, D. J. Saunders, J. Nunn, I. A. Walmisley, R. Uzdin, and E. Poem, Experimental demonstration of quantum effects in the operation of microscopic heat engines, *Phys. Rev. Lett.* **122**, 110601 (2019).
- [9] M. Horodecki and J. Oppenheim, Fundamental limitations for quantum and nanoscale thermodynamics, *Nat. Commun.* **4**, 2059 (2013).
- [10] M. O. Scully, M. S. Zubairy, G. S. Agarwal, and H. Walther, Extracting work from a single heat bath via vanishing quantum coherence, *Science* **299**, 862 (2003).
- [11] P. Kammerlander and J. Anders, Coherence and measurement in quantum thermodynamics, *Sci. Rep.* **6**, 22174 (2016).
- [12] K. Korzekwa, M. Lostaglio, J. Oppenheim, and D. Jennings, The extraction of work from quantum coherence, *New J. Phys.* **18**, 023045 (2016).
- [13] G. Francica, F. C. Binder, G. Guarnieri, M. T. Mitchison, J. Goold, and F. Plastina, Quantum coherence and ergotropy, *Phys. Rev. Lett.* **125**, 180603 (2020).
- [14] F. G. S. L. Brandão, M. Horodecki, J. Oppenheim, J. M. Renes, and R. W. Spekkens, Resource theory of quantum states out of thermal equilibrium, *Phys. Rev. Lett.* **111**, 250404 (2013).
- [15] E. Chitambar and G. Gour, Quantum resource theories, *Rev. Mod. Phys.* **91**, 025001 (2019).
- [16] M. A. Ciampini, L. Mancino, A. Orioux, C. Vigliar, P. Mataloni, M. Paternostro, and M. Barbieri, Experimental extractable work-based multipartite separability criteria, *npj Quantum Inf.* **3**, 10 (2017).
- [17] J. Millen and A. Xuereb, Perspective on quantum thermodynamics, *New J. Phys.* **18**, 011002 (2016).
- [18] L. M. Cangemi, C. Bhadra, and A. Levy, Quantum engines and refrigerators, arXiv:2302.00726 (2023).
- [19] I. Bloch, J. Dalibard, and S. Nascimbéne, Quantum simulations with ultracold quantum gases, *Nature Phys.* **8**, 267 (2012).
- [20] T. Langen, R. Geiger, and J. Schmiedmayer, Ultracold atoms out of equilibrium, *Annu. Rev. Condens. Matter Phys.* **6**, 201 (2015).
- [21] N. M. Myers, F. J. Peña, O. Negrete, P. Vargas, G. De Chiara, and S. Deffner, Boosting engine performance with Bose-Einstein condensation, *New J. Phys.* **24**, 025001 (2022).
- [22] J. Jaramillo, M. Beau, and A. del Campo, Quantum supremacy of many-particle thermal machines, *New J. Phys.* **18**, 075019 (2016).
- [23] T. Fogarty and T. Busch, A many-body heat engine at criticality, *Quantum Sci. Technol.* **6**, 015003 (2020).
- [24] E. Q. Simmons, R. Sajjad, K. Keithley, H. Mas, J. L. Tanlimco, E. Nolasco-Martinez, Y. Bai, G. H. Fredrickson, and D. M. Weld, Thermodynamic engine with a quantum degenerate working fluid, *Phys. Rev. Res.* **5**, L042009 (2023).
- [25] J. Koch, K. Menon, E. Cuestas, S. Barbosa, E. Lutz, T. Fogarty, T. Busch, and A. Widera, A quantum engine in the BEC-BCS crossover, *Nature* **621**, 723 (2023).
- [26] J. Bengtsson, M. N. Tengstrand, A. Wacker, P. Samuelsson, M. Ueda, H. Linke, and S. M. Reimann, Quantum Szilard engine with attractively interacting bosons, *Phys. Rev. Lett.* **120**, 100601 (2018).
- [27] M. Boubakour, T. Fogarty, and T. Busch, Interaction-enhanced quantum heat engine, *Phys. Rev. Res.* **5**, 013088 (2023).
- [28] Y.-Y. Chen, G. Watanabe, Y.-C. Yu, X.-W. Guan, and A. del Campo, An interaction-driven many-particle quantum heat engine and its universal behavior, *npj Quantum Inf.* **5**, 88 (2019).
- [29] R. Watson and K. Kheruntsyan, An interaction-driven quantum many-body engine enabled by atom-atom correlations, arXiv:2308.05266 (2023).
- [30] G.-B. Jo, Y. Shin, S. Will, T. A. Pasquini, M. Saba, W. Ketterle, D. E. Pritchard, M. Vengalattore, and

- M. Prentiss, Long phase coherence time and number squeezing of two Bose-Einstein condensates on an atom chip, *Phys. Rev. Lett.* **98**, 030407 (2007).
- [31] C. Orzel, A. Tuchman, M. Fenselau, M. Yasuda, and M. Kasevich, Squeezed states in a Bose-Einstein condensate, *Science* **291**, 2386 (2001).
- [32] A. Sørensen, L.-M. Duan, J. I. Cirac, and P. Zoller, Many-particle entanglement with Bose-Einstein condensates, *Nature* **409**, 63 (2001).
- [33] J. Estève, C. Gross, A. Weller, S. Giovanazzi, and M. K. Oberthaler, Squeezing and entanglement in a Bose-Einstein condensate, *Nature* **455**, 1216 (2008).
- [34] W. Muessel, H. Strobel, D. Linnemann, D. B. Hume, and M. K. Oberthaler, Scalable spin squeezing for quantum-enhanced magnetometry with Bose-Einstein condensates, *Phys. Rev. Lett.* **113**, 103004 (2014).
- [35] L. Pezzè, A. Smerzi, M. K. Oberthaler, R. Schmied, and P. Treutlein, Quantum metrology with nonclassical states of atomic ensembles, *Rev. Mod. Phys.* **90**, 035005 (2018).
- [36] S. S. Szigeti, S. P. Nolan, J. D. Close, and S. A. Haine, High-precision quantum-enhanced gravimetry with a Bose-Einstein condensate, *Phys. Rev. Lett.* **125**, 100402 (2020).
- [37] A. Polkovnikov, Microscopic diagonal entropy and its connection to basic thermodynamic relations, *Ann. Phys.* **326**, 486 (2011).
- [38] L. F. Santos, A. Polkovnikov, and M. Rigol, Entropy of isolated quantum systems after a quench, *Phys. Rev. Lett.* **107**, 040601 (2011).
- [39] W. Pusz and S. L. Woronowicz, Passive states and KMS states for general quantum systems, *Communications in Mathematical Physics* **58**, 273 (1978).
- [40] R. Kosloff and Y. Rezek, The quantum harmonic Otto cycle, *Entropy* **19**, 136 (2017).
- [41] R. Balian, Gain of information in a quantum measurement, *Eur. J. Phys.* **10**, 208 (1989).
- [42] M. Esposito and C. Van den Broeck, Second law and Landauer principle far from equilibrium, *EPL* **95**, 40004 (2011).
- [43] T. Baumgratz, M. Cramer, and M. B. Plenio, Quantifying coherence, *Phys. Rev. Lett.* **113**, 140401 (2014).
- [44] H. T. Quan, Y.-x. Liu, C. P. Sun, and F. Nori, Quantum thermodynamic cycles and quantum heat engines, *Phys. Rev. E* **76**, 031105 (2007).
- [45] F. Plastina, A. Alecce, T. J. G. Apollaro, G. Falcone, G. Francica, F. Galve, N. Lo Gullo, and R. Zambrini, Irreversible work and inner friction in quantum thermodynamic processes, *Phys. Rev. Lett.* **113**, 260601 (2014).
- [46] A. J. Leggett, Bose-Einstein condensation in the alkali gases: Some fundamental concepts, *Rev. Mod. Phys.* **73**, 307 (2001).
- [47] M. Albiez, R. Gati, J. Fölling, S. Hunsmann, M. Cristiani, and M. K. Oberthaler, Direct observation of tunneling and nonlinear self-trapping in a single bosonic Josephson junction, *Phys. Rev. Lett.* **95**, 010402 (2005).
- [48] M. R. Matthews, D. S. Hall, D. S. Jin, J. R. Ensher, C. E. Wieman, E. A. Cornell, F. Dalfovo, C. Minniti, and S. Stringari, Dynamical response of a Bose-Einstein condensate to a discontinuous change in internal state, *Phys. Rev. Lett.* **81**, 243 (1998).
- [49] D. S. Hall, J. R. Ensher, D. S. Jin, M. R. Matthews, C. E. Wieman, and E. A. Cornell, Recent experiments with Bose-condensed gases at JILA, in *Methods for UL-trasensitive Detection*, Vol. 3270, edited by B. L. Fearey, International Society for Optics and Photonics (SPIE, 1998) pp. 98 – 106.
- [50] M. H. Anderson, J. R. Ensher, M. R. Matthews, C. E. Wieman, and E. A. Cornell, Observation of Bose-Einstein condensation in a dilute atomic vapor, *Science* **269**, 198 (1995).
- [51] K. B. Davis, M. O. Mewes, M. R. Andrews, N. J. van Druten, D. S. Durfee, D. M. Kurn, and W. Ketterle, Bose-Einstein condensation in a gas of sodium atoms, *Phys. Rev. Lett.* **75**, 3969 (1995).
- [52] W. Ketterle, D. S. Durfee, and D. M. Stamper-Kurn, Making, probing and understanding Bose-Einstein condensates, in *Bose-Einstein Condensation in Atomic Gases*, Proceedings of the International School of Physics “Enrico Fermi”, Vol. 140 (IOS Press, 1999) pp. 67–176.
- [53] F. Dalfovo, S. Giorgini, L. P. Pitaevskii, and S. Stringari, Theory of Bose-Einstein condensation in trapped gases, *Rev. Mod. Phys.* **71**, 463 (1999).
- [54] J. Radcliffe, Some properties of coherent spin states, *J. Phys. A: Gen. Phys.* **4**, 313 (1971).
- [55] T. Holstein and H. Primakoff, Field dependence of the intrinsic domain magnetization of a ferromagnet, *Phys. Rev.* **58**, 1098 (1940).
- [56] R. J. Glauber, Coherent and incoherent states of the radiation field, *Phys. Rev.* **131**, 2766 (1963).
- [57] G. J. Milburn, J. Corney, E. M. Wright, and D. F. Walls, Quantum dynamics of an atomic Bose-Einstein condensate in a double-well potential, *Phys. Rev. A* **55**, 4318 (1997).
- [58] S. Raghavan, A. Smerzi, S. Fantoni, and S. R. Shenoy, Coherent oscillations between two weakly coupled Bose-Einstein condensates: Josephson effects, π oscillations, and macroscopic quantum self-trapping, *Phys. Rev. A* **59**, 620 (1999).
- [59] R. Gati and M. K. Oberthaler, A bosonic Josephson junction, *J. Phys. B: At. Mol. Opt. Phys.* **40**, R61 (2007).
- [60] M. R. Matthews, B. P. Anderson, P. C. Haljan, D. S. Hall, M. J. Holland, J. E. Williams, C. E. Wieman, and E. A. Cornell, Watching a superfluid untwist itself: Recurrence of Rabi oscillations in a Bose-Einstein condensate, *Phys. Rev. Lett.* **83**, 3358 (1999).
- [61] T. Zibold, E. Nicklas, C. Gross, and M. K. Oberthaler, Classical bifurcation at the transition from Rabi to Josephson dynamics, *Phys. Rev. Lett.* **105**, 204101 (2010).
- [62] J. Javanainen and S. M. Yoo, Quantum phase of a Bose-Einstein condensate with an arbitrary number of atoms, *Phys. Rev. Lett.* **76**, 161 (1996).
- [63] J. I. Cirac, C. W. Gardiner, M. Naraschewski, and P. Zoller, Continuous observation of interference fringes from Bose condensates, *Phys. Rev. A* **54**, R3714 (1996).
- [64] Y. Castin and J. Dalibard, Relative phase of two Bose-Einstein condensates, *Phys. Rev. A* **55**, 4330 (1997).
- [65] S. Barnett, K. Burnett, and J. Vaccaro, Why a condensate can be thought of as having a definite phase, *J. Res. Natl. Inst. Stand. Technol.* **101**, 593 (1996).
- [66] M. Andrews, C. Townsend, H.-J. Miesner, D. Durfee, D. Kurn, and W. Ketterle, Observation of interference between two Bose condensates, *Science* **275**, 637 (1997).
- [67] D. S. Hall, M. R. Matthews, C. E. Wieman, and E. A. Cornell, Measurements of relative phase in two-

- component Bose-Einstein condensates, *Phys. Rev. Lett.* **81**, 1543 (1998).
- [68] M. A. Kasevich, Coherence with atoms, *Science* **298**, 1363 (2002).
- [69] P. Carruthers and M. M. Nieto, Coherent states and the number-phase uncertainty relation, *Phys. Rev. Lett.* **14**, 387 (1965).
- [70] V. Bužek, A. D. Wilson-Gordon, P. L. Knight, and W. K. Lai, Coherent states in a finite-dimensional basis: Their phase properties and relationship to coherent states of light, *Phys. Rev. A* **45**, 8079 (1992).
- [71] L. Simon and W. T. Strunz, Analytical results for Josephson dynamics of ultracold bosons, *Phys. Rev. A* **86**, 053625 (2012).
- [72] S. B. Papp, J. M. Pino, and C. E. Wieman, Tunable miscibility in a dual-species Bose-Einstein condensate, *Phys. Rev. Lett.* **101**, 040402 (2008).
- [73] S. Tojo, Y. Taguchi, Y. Masuyama, T. Hayashi, H. Saito, and T. Hirano, Controlling phase separation of binary Bose-Einstein condensates via mixed-spin-channel Feshbach resonance, *Phys. Rev. A* **82**, 033609 (2010).
- [74] C. Chin, R. Grimm, P. Julienne, and E. Tiesinga, Feshbach resonances in ultracold gases, *Rev. Mod. Phys.* **82**, 1225 (2010).
- [75] M. Mohammady, A. Auffèves, and J. Anders, Energetic footprints of irreversibility in the quantum regime, *Commun. Phys.* **3**, 89 (2020).
- [76] R. J. Glauber, The quantum theory of optical coherence, *Phys. Rev.* **130**, 2529 (1963).
- [77] R. Landauer, Irreversibility and heat generation in the computing process, *IBM J. Res. Dev.* **5**, 183 (1961).
- [78] S. Yang and S. John, Coherence and antibunching in a trapped interacting Bose-Einstein condensate, *Phys. Rev. B* **84**, 024515 (2011).
- [79] Also known as the Lambert W -function, denoted by W_k . We avoid this notation to avoid confusion with work output.
- [80] R. M. Corless, G. H. Gonnet, D. E. Hare, D. J. Jeffrey, and D. E. Knuth, On the Lambert W function, *Adv. Comput. Math.* **5**, 329 (1996).
- [81] J. Ma, X. Wang, C.-P. Sun, and F. Nori, Quantum spin squeezing, *Phys. Rep.* **509**, 89 (2011).
- [82] M. Kitagawa and M. Ueda, Squeezed spin states, *Phys. Rev. A* **47**, 5138 (1993).
- [83] X. Wang and B. C. Sanders, Relations between bosonic quadrature squeezing and atomic spin squeezing, *Phys. Rev. A* **68**, 033821 (2003).
- [84] L.-M. Duan, A. Sørensen, J. I. Cirac, and P. Zoller, Squeezing and entanglement of atomic beams, *Phys. Rev. Lett.* **85**, 3991 (2000).
- [85] H. Pu and P. Meystre, Creating macroscopic atomic Einstein-Podolsky-Rosen states from Bose-Einstein condensates, *Phys. Rev. Lett.* **85**, 3987 (2000).
- [86] C. Gross, H. Strobel, E. Nicklas, T. Zibold, N. Bargill, G. Kurizki, and M. K. Oberthaler, Atomic homodyne detection of continuous-variable entangled twin-atom states, *Nature* **480**, 219 (2011).
- [87] D. Stoler, Equivalence classes of minimum uncertainty packets, *Phys. Rev. D* **1**, 3217 (1970).
- [88] H. P. Yuen, Two-photon coherent states of the radiation field, *Phys. Rev. A* **13**, 2226 (1976).
- [89] C. M. Caves, Quantum-mechanical noise in an interferometer, *Phys. Rev. D* **23**, 1693 (1981).
- [90] C. C. Gerry and P. L. Knight, *Introductory quantum optics* (Cambridge University Press, New York, 2005).
- [91] J. J. Gong and P. K. Aravind, Expansion coefficients of a squeezed coherent state in the number state basis, *Am. J. Phys.* **58**, 1003 (1990).
- [92] R. S. Bondurant and J. H. Shapiro, Squeezed states in phase-sensing interferometers, *Phys. Rev. D* **30**, 2548 (1984).
- [93] W. Schleich and J. Wheeler, Oscillations in photon distribution of squeezed states and interference in phase space, *Nature* **326**, 574 (1987).
- [94] W. Schleich and J. Wheeler, Oscillations in photon distribution of squeezed states, *J. Opt. Soc. Am. B* **4**, 1715 (1987).
- [95] The change of sign of W_{class} means that there is value of $\langle \hat{n} \rangle$ where $W_{\text{class}} = 0$ despite differences in the squeezed and thermal distributions. The choice of squeezing parameters can possibly be optimised to find similar “serendipitous” points of zero or small W_{class} for other values of $\langle \hat{n} \rangle$.
- [96] M. Perarnau-Llobet, K. V. Hovhannisyanyan, M. Huber, P. Skrzypczyk, N. Brunner, and A. Acín, Extractable work from correlations, *Phys. Rev. X* **5**, 041011 (2015).
- [97] F. Sapienza, F. Cerisola, and A. J. Roncaglia, Correlations as a resource in quantum thermodynamics, *Nat. Commun.* **10**, 2492 (2019).
- [98] A. Touil, B. Çakmak, and S. Deffner, Ergotropy from quantum and classical correlations, *J. Phys. A: Math. Theor.* **55**, 025301 (2021).
- [99] G. Francica, J. Goold, F. Plastina, and M. Paternostro, Daemonic ergotropy: enhanced work extraction from quantum correlations, *npj Quantum Inf.* **3**, 12 (2017).
- [100] C. H. Bennett, H. J. Bernstein, S. Popescu, and B. Schumacher, Concentrating partial entanglement by local operations, *Phys. Rev. A* **53**, 2046 (1996).
- [101] A. S. Sørensen and K. Mølmer, Entanglement and extreme spin squeezing, *Phys. Rev. Lett.* **86**, 4431 (2001).
- [102] G. Modugno, G. Ferrari, G. Roati, R. J. Brecha, A. Simoni, and M. Inguscio, Bose-Einstein condensation of potassium atoms by sympathetic cooling, *Science* **294**, 1320 (2001).
- [103] H. Grabert and U. Weiss, Quantum tunneling rates for asymmetric double-well systems with Ohmic dissipation, *Phys. Rev. Lett.* **54**, 1605 (1985).
- [104] M. P. A. Fisher and A. T. Dorsey, Dissipative quantum tunneling in a biased double-well system at finite temperatures, *Phys. Rev. Lett.* **54**, 1609 (1985).
- [105] A. S. Bradley and P. B. Blakie, Stochastic projected Gross-Pitaevskii equation for spinor and multicomponent condensates, *Phys. Rev. A* **90**, 023631 (2014).
- [106] Y. Kawaguchi and M. Ueda, Spinor Bose-Einstein condensates, *Phys. Rep.* **520**, 253 (2012).
- [107] D. M. Stamper-Kurn and M. Ueda, Spinor Bose gases: Symmetries, magnetism, and quantum dynamics, *Rev. Mod. Phys.* **85**, 1191 (2013).
- [108] Q. Bouton, J. Nettersheim, S. Burgardt, D. Adam, E. Lutz, and A. Widera, A quantum heat engine driven by atomic collisions, *Nat. Commun.* **12**, 2063 (2021).
- [109] V. V. Ulyanov and O. B. Zaslavskii, New methods in the theory of quantum spin systems, *Phys. Rep.* **216**, 179 (1992).
- [110] K. Hammerer, A. S. Sørensen, and E. S. Polzik, Quantum interface between light and atomic ensembles, *Rev. Mod. Phys.* **82**, 1041 (2010).

- [111] I. D. Leroux, M. H. Schleier-Smith, and V. Vuletić, Implementation of cavity squeezing of a collective atomic spin, *Phys. Rev. Lett.* **104**, 073602 (2010).
- [112] I. Bouchoule and K. Mølmer, Spin squeezing of atoms by the dipole interaction in virtually excited Rydberg states, *Phys. Rev. A* **65**, 041803 (2002).
- [113] M. Saffman, T. G. Walker, and K. Mølmer, Quantum information with Rydberg atoms, *Rev. Mod. Phys.* **82**, 2313 (2010).
- [114] A. Sørensen and K. Mølmer, Entanglement and quantum computation with ions in thermal motion, *Phys. Rev. A* **62**, 022311 (2000).
- [115] V. Meyer, M. A. Rowe, D. Kielpinski, C. A. Sackett, W. M. Itano, C. Monroe, and D. J. Wineland, Experimental demonstration of entanglement-enhanced rotation angle estimation using trapped ions, *Phys. Rev. Lett.* **86**, 5870 (2001).
- [116] J. Klaers, F. Vewinger, and M. Weitz, Thermalization of a two-dimensional photonic gas in a ‘white wall’ photon box, *Nature Phys.* **6**, 512 (2010).
- [117] J. Klaers, J. Schmitt, F. Vewinger, and M. Weitz, Bose-Einstein condensation of photons in an optical microcavity, *Nature* **468**, 545 (2010).
- [118] M. Kitagawa and Y. Yamamoto, Number-phase minimum-uncertainty state with reduced number uncertainty in a kerr nonlinear interferometer, *Phys. Rev. A* **34**, 3974 (1986).
- [119] M. Walschaers, Non-gaussian quantum states and where to find them, *PRX Quantum* **2**, 030204 (2021).
- [120] A. Erdélyi, *Higher Transcendental Functions*, Vol. II (McGraw-Hill, New York, 1953).
- [121] B. F. Bunck, A fast algorithm for evaluation of normalized Hermite functions, *Bit Numer Math* **49**, 281 (2009).